Available online at www.sciencedirect.com
SCIENCE DIRECT®
Applied Catalysis B: Environmental 49 (2004) 159–171
APPLIED CATALYSIS B: ENVIRONMENTAL
www.elsevier.com/locate/apcatb

Mechanism of the selective catalytic reduction of NO_x by C_2H_5OH over Ag/Al_2O_3

Yunbo Yu, Hong He*, Qingcai Feng, Hongwei Gao, Xin Yang

Research Center for Eco-Environmental Sciences, Chinese Academy of Sciences, Beijing 100085, China

Received 30 June 2003; received in revised form 2 December 2003; accepted 8 December 2003

Abstract

The mechanism of the selective catalytic reduction (SCR) of NO_x by C_2H_5OH over silver catalyst (Ag/Al_2O_3) was investigated using in situ diffuse reflectance infrared Fourier transform spectroscopy (DRIFTS). Attention was focused on the formation and reactivity of novel enolic species on the Ag/Al_2O_3 surface. DRIFTS spectra show that the surface enolic species, which was derived from partial oxidation of C_2H_5OH over Ag/Al_2O_3 in the presence of excess oxygen, play a crucial role in the formation of isocynate species (NCO) by reaction with $NO + O_2$ or NO_3^- absorbed on the surface of Ag/Al_2O_3. 2,3-dihydrofuran was used to an enolic model compound in our DRITFS study, and the results support our assignment. A novel mechanism of the SCR of NO_x by C_2H_5OH is proposed based on the DRIFTS studies. The mechanistic differences between the SCR of NO_x by C_2H_5OH and that by C_3H_6 are discussed. The high reactivity of the enolic species results in high surface concentration of NCO and high efficiency of NO_x reduction using C_2H_5OH as a reductant. The results of density functional theory (DFT) calculations are in good agreement with the DRIFTS spectra, and support our suggestions about the surface enolic species.

Keywords: Selective catalytic reduction (SCR); NO_x; In situ DRIFTS; Alumina supported silver; C_2H_5OH; Enolic species; Acetate; Density functional theory (DFT) calculations

1. Introduction

Alumina supported silver catalyst (Ag/Al_2O_3) has been studied as a promising catalyst due to its high activity for the selective catalytic reduction (SCR) of NO_x by hydrocarbons and oxygenated hydrocarbons in the presence of excess oxygen [1–12]. In particular, C_2H_5OH is extremely effective for the SCR of NO_x over Ag/Al_2O_3 [1,5].

The adsorbed species on catalysts during the SCR of NO_x have been observed by many researchers using IR spectroscopy, and several intermediates have been proposed to take part in the reduction of NO_x, such as NO_3^- [4,8,12], CH_3COO^- [9,12,13], R–NO_2 [7,9,13], R–ONO [7,9,13], and NCO [4,5,8,13,14]. IR spectra have shown that adsorbed nitrates (NO_3^-) and acetate (CH_3COO^-) were the predominant surface species during the SCR of NO_x on Al_2O_3 or Ag/Al_2O_3 [8,12,15,16]. Based on our previous IR studies [4,5], isocyanate species (NCO) was detected respectively on Ag and Al sites by adsorption and reaction of $NO + O_2 +$ C_2H_5OH or C_3H_6 on Ag/Al_2O_3 surface in a vacuum system. It was suggested that NCO species on the surface would be a crucial intermediate in the NO_x reduction process over an Ag/Al_2O_3 catalyst. Some organo-nitro and organo-nitrite compounds such as R–NO_2 and R–ONO have been observed as the precursors of NCO species [4,5]. Ukisu et al. [17,18] and Kameoka et al. [14,19] also reported that NCO species was a vital intermediate for the SCR of NO_x, and suggested that the high productivity of NCO species resulted in a high efficiency of NO_x reduction by C_2H_5OH or hydrocarbons. Recently, strongly adsorbed species such as nitrates and acetate were proposed to be key intermediates in the formation of organo-nitro and organo-nitrite compounds [12,13].

On the basis of these findings, a possible mechanism for the SCR of NO_x by C_2H_5OH over Ag/Al_2O_3 was considered as similar to that of C_3H_6, approximately, $NO + O_2 + C_2H_5OH \rightarrow NO_x$ (nitrate in particular) $+ C_xH_yO_z$ (acetate in particular) $\rightarrow$ R–NO_2 + R–ONO $\rightarrow$ –NCO + –CN + NO + O_2 $\rightarrow N_2$ [13,20]. However, this mechanism does not sufficiently explain why C_2H_5OH has a higher efficiency for the SCR of NO_x over Ag/Al_2O_3 than hydrocarbons such as C_3H_6.

In this paper, the formation and dynamic performance of partial oxidation products of C_2H_5OH and C_3H_6 over

* Corresponding author. Tel.: +86-10-62849123; fax: +86-10-62849123.
E-mail address: honghe@mail.rcees.ac.cn (H. He).

0926-3373/$ – see front matter © 2003 Elsevier B.V. All rights reserved.
doi:10.1016/j.apcatb.2003.12.004

Ag/Al_2O_3 were studied by an in situ DRIFTS method. The most significant observation is that enolic species, formed from the partial oxidation of C_2H_5OH and C_3H_6 over Ag/Al_2O_3, have high reactivity with $NO + O_2$ to form NCO. Finally, we propose a possible reaction scheme to explain the high efficiency of the NO_x reduction by C_2H_5OH.

2. Experimental and theoretical

An Ag/Al_2O_3 catalyst (Ag loading is 5 wt.%) was prepared by an impregnation method described in our earlier paper [21]. The catalytic activity was measured in a fixed-bed reactor by passing a gaseous mixture of NO 800 ppm, reductant C_3H_6 1714 ppm, or C_2H_5OH 1565 ppm, or CH_3CHO 1565 ppm, or CH_3COOH 1565 ppm, water vapor (10%), and O_2 (10%) in N_2 balance at a total flow rate of 4000 ml min^{-1} (GHSV = 50,000 h^{-1}). NO_x conversion was analyzed on-line by a chemiluminescence $NO/NO_2/NO_x$ analyzer (42C-hl, Thermo Environmental). An aqueous C_2H_5OH (or CH_3CHO, or CH_3COOH) solution was supplied with a micropump into the gas stream and vaporized by a coiled heater at the inlet of the reactor.

In situ diffuse reflectance infrared Fourier transform spectroscopy (DRIFTS) spectra were recorded on a Nexus 670 (Thermo Nicolet) FT-IR, equipped with an in situ diffuse reflection chamber and a high sensitivity MCT detector. The Ag/Al_2O_3 catalyst for the in situ DRIFTS studies was finely ground and placed into a ceramic crucible in the in situ chamber. Mass flow controllers and a sample temperature controller were used to simulate the real reaction conditions, which are the same as those in the catalytic activity test, such as mixture of gases, pressure, and sample temperature. Prior to recording each DRIFTS spectrum, the Ag/Al_2O_3 catalyst was heated in situ in (10%) O_2/N_2 flow at 873 K for 1 h, then cooled to the desired temperature for taking a reference spectrum. All spectra reported here were taken at a resolution of 4 cm^{-1} for 100 scans.

Density functional theory (DFT) calculation was used to confirm the structure of surface enolic species on Ag/Al_2O_3 using the GAUSSIAN 98 suite of programs. The LANL2DZ basis set was employed to carry out the DFT-B3P86 (Becke's three parameter function with a non-local correlation provided by the Perdew 86 expression) calculations. The calculated vibration frequencies and infrared intensity of the vibrational normal modes were picked up by the Hyperchem^{TM} Version 6.0 package.

3. Results

3.1. Reaction activity of various organic compounds for the SCR of NO_x over Ag/Al_2O_3

Fig. 1 shows the reaction activity of various organic compounds for the SCR of NO_x over Ag/Al_2O_3. When using C_2H_5OH as a reductant, the maximal conversion of NO_x is up to 98.7%, and the average conversion of NO_x is ca. 90% even in the wide temperature range of 578–883 K. In the case of CH_3CHO, it is worthwhile to note that the NO_x conversion is nearly the same as that of C_2H_5OH at temperatures below 766 K. Compared with C_2H_5OH and CH_3CHO, there is a relatively lower NO_x conversion by C_3H_6 in the whole reaction temperature range, especially in the low temperature range. However, when using CH_3COOH as a reductant with the same carbon atom concentration (ppm C), the highest conversion of NO_x is only 58%. These results indicate that the NO_x conversion is strongly influenced by the kind of reductant, and the order of the reaction activity is C_2H_5OH (CH_3CHO)> C_3H_6 > CH_3COOH. In other words, partially oxidized hydrocarbons such as C_2H_5OH and CH_3CHO are extremely efficient for the NO_x reduction, while deep oxidization of hydrocarbons lowers NO_x conversion.

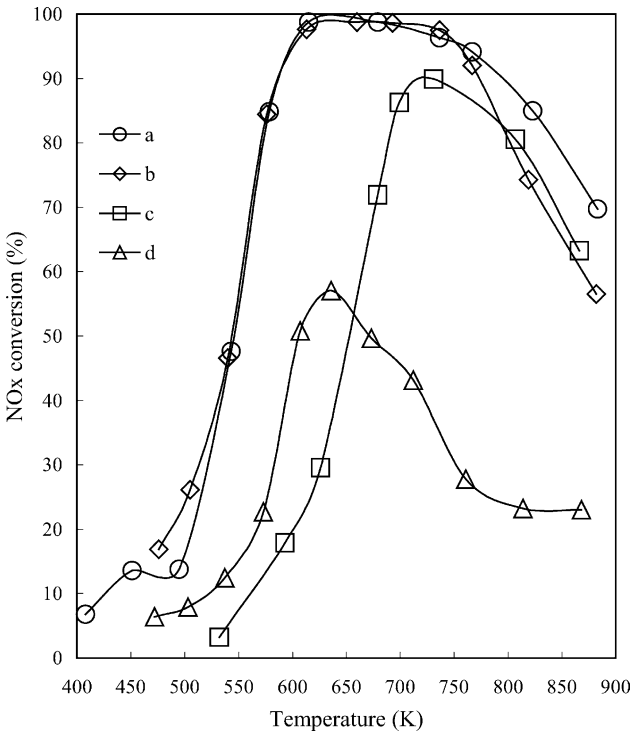

Fig. 1. Activity of Ag/Al_2O_3 for the SCR of NO_x by various reductants. Conditions: NO, 800 ppm; O_2, 10%; H_2O, 10% and reductants (a) C_2H_5OH, 1565 ppm, (b) CH_3CHO, 1565 ppm, (c) C_3H_6, 1714 ppm, and (d) CH_3COOH, 1565 ppm, N_2 balance, GHSV = 50,000 h^{-1}.

3.2. Steady state in situ DRIFTS study of the SCR of NO_x by C_2H_5OH over Ag/Al_2O_3

The difference of these reductants for the SCR of NO_x over the Ag/Al_2O_3 was investigated using DRIFTS. Fig. 2 shows the in situ DRIFTS spectra of Ag/Al_2O_3 during the reaction of NO 800 ppm + C_2H_5OH 1565 ppm + O_2 (10%) at a temperature range of 473–823 K in steady states, together with a spectrum recorded at 473 K in a flow of NO 800 ppm + O_2 (10%). After an exposure of the Ag/Al_2O_3

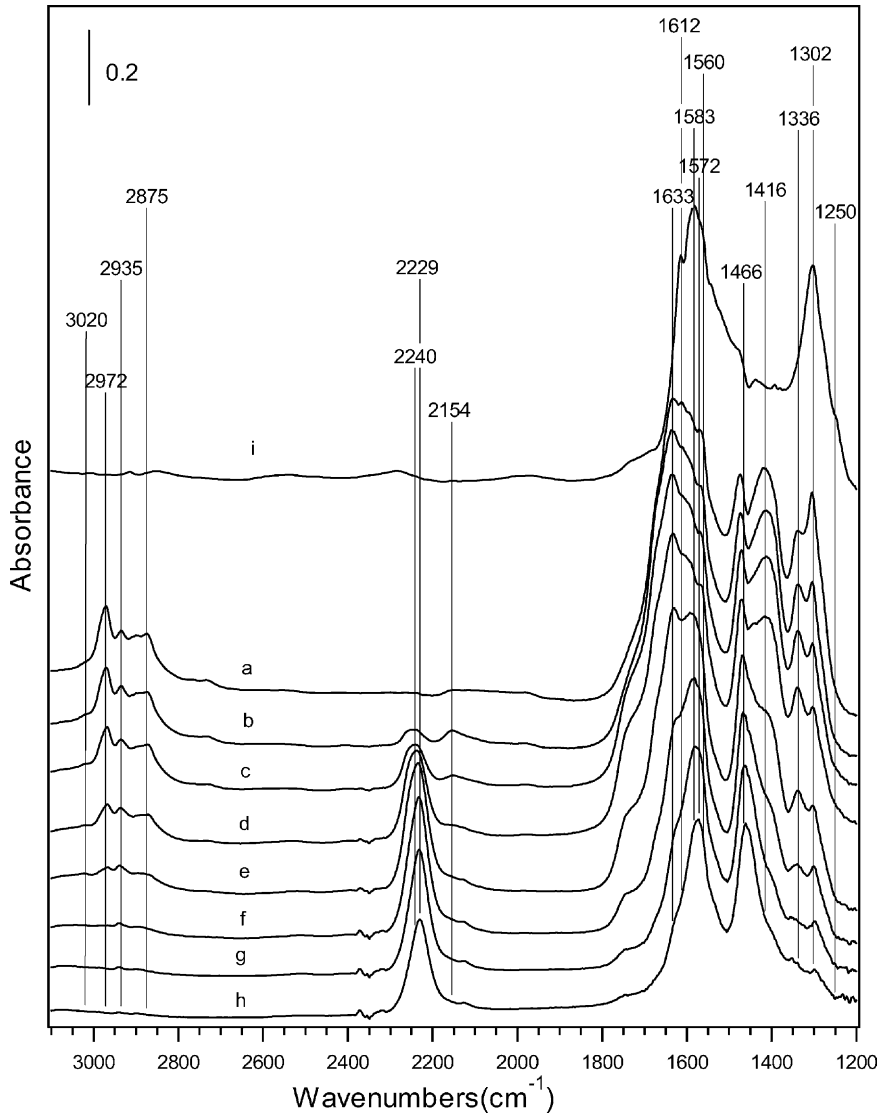

Fig. 2. DRIFTS spectra of adsorbed species in the steady state over Ag/Al_2O_3 in the flow of $NO + C_2H_5OH + O_2$ at (a) 473 K, (b) 523 K, (c) 573 K, (d) 623 K, (e) 673 K, (f) 723 K, (g) 773 K, (h) 823 K, and (i) $NO + O_2$ for 120 min at 473 K. Conditions: NO, 800 ppm; C_2H_5OH, 1565 ppm; O_2, 10%.

to $NO + O_2$ for 120 min (spectrum i), strong peaks at 1583, 1302 cm^{-1} and shoulders at 1612, 1560, and 1250 cm^{-1} were observed, which were respectively assigned to unidenate (1560, 1250 cm^{-1}), bidentate (1583, 1302 cm^{-1}), and bridging (1612 cm^{-1}) nitrates according to the literature [8,12].

During the $NO+C_2H_5OH+O_2$ reaction at various temperatures (473–823 K) in steady states over Ag/Al_2O_3 (spectra a–h), the peaks of nitrates mentioned above also appeared. We also detected strong peaks at 1572 and 1466 cm^{-1}. These peaks were attributed to ν_{as}(OCO), and ν_s(OCO) of adsorbed acetate respectively, because the frequencies of these peaks are in good agreement with those of CH_3COOH adsorbed on Ag/Al_2O_3 (this result not shown) and alumina [16,22]. It is interesting to note that, at low temperature region 473–673 K (spectra a–e), the peak at 1633 cm^{-1} is predominant, accompanied by the appearance of strong peaks at 1416 and 1336 cm^{-1}. The three peaks were also observed on Ag/Al_2O_3 during the oxidation of C_2H_5OH and CH_3CHO, and were attributed to a surface enolic species according to our earlier study [21]. More evidences of the assignment for these peaks will be discussed below.

In the region of 2300–2000 cm^{-1}, a strong peak at 2240 cm^{-1} at 623 K (spectrum c) was observed and shifted to 2229 cm^{-1} at 673 K (spectrum e) during the SCR of NO_x over Ag/Al_2O_3, which was assigned to NCO bound to the Al site (2240 cm^{-1}) and Ag site (2229 cm^{-1}) [4,5,8,14,17,18]. In addition, another weak peak at 2154 cm^{-1} was due to CN [4,23].

In the region of 3100–2800 cm^{-1}, peaks at 2972 and 2875 cm^{-1} were assigned to ν_{as}(C–H) and ν_s(C–H) of $-CH_3$ [4,24], and the peak at 2935 cm^{-1} was possibly due to ν_{as}(C–H) of methylene [24]. In addition, a very weak peak at 3020 cm^{-1} was observed, which is the characteristic of C–H stretching vibration model in C=CH group [24,25].

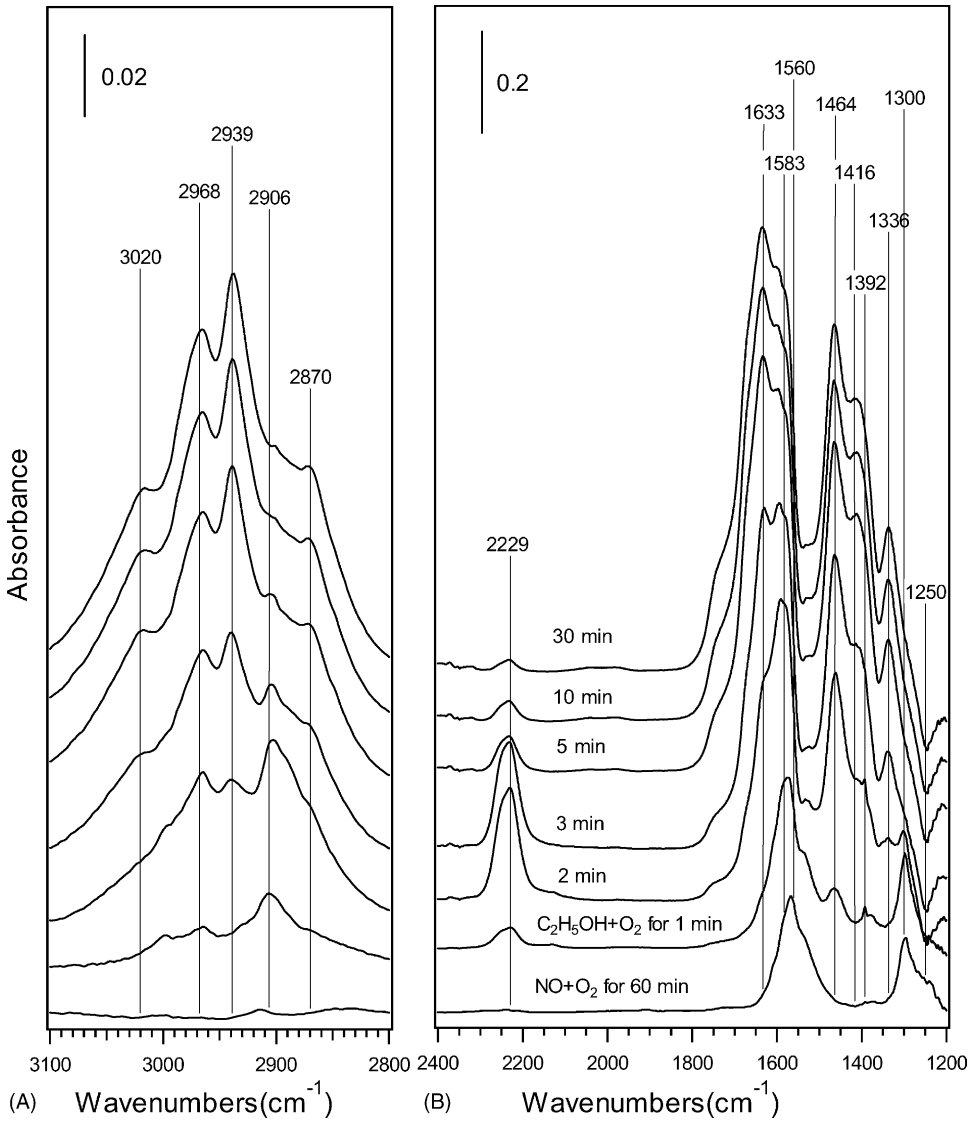

Fig. 3. Dynamic changes of in situ DRIFTS spectra over Ag/Al_2O_3 as a function of time in a flow of $C_2H_5OH + O_2$ at 673 K. Before the measurement, the catalyst was pre-exposed to a flow of $NO + O_2$ for 60 min at 673 K. Conditions: NO, 800 ppm; C_2H_5OH, 1565 ppm; O_2, 10%.

From a comparison of the intensity of each peak, it is considered that the acetate surface species is predominant within a high temperature range of 773–873 K, while at a low temperature range of 473–673 K, the enolic species and nitrates become dominant on the Ag/Al_2O_3 surface.

3.3. Reactivity of adsorbed NO_3^- over Ag/Al_2O_3

The reactivity of the nitrates toward $C_2H_5OH + O_2$ and $C_3H_6 + O_2$ was studied by the transient response of DRIFTS method. Fig. 3A and B show the in situ DRIFTS spectra of Ag/Al_2O_3 in a flow of C_2H_5OH 1565 ppm + O_2 (10%) after the catalyst was pre-exposed to a flow of NO 800 ppm + O_2 (10%) for 60 min at 673 K. Switching the fed gas from $NO + O_2$ to $C_2H_5OH + O_2$ led to a drastic decrease in the intensity of nitrate peaks (1250 and 1300 cm^{-1}), and they disappeared completely after 3 min. Simultaneously, the intensity of the peak at 2229 cm^{-1} due to NCO sharply increased initially, reached a maximum after 3 min, and then decreased gradually. This indicates that the nitrates are highly active for reaction with $C_2H_5OH + O_2$ to form NCO.

The same set of experiments was also performed with C_3H_6 as a reductant, and the dynamic changes of DRIFTS spectra as a function of time are shown in Fig. 4. Compared with Fig. 3, the disappearance rate of nitrate peaks at 1245 and 1300 cm^{-1} dramatically slowed down, as did the increase rate of NCO peak, indicating that C_3H_6 is not as active as C_2H_5OH for reaction with nitrate to form NCO.

3.4. Formation and reactivity of partial oxidation products of C_2H_5OH, CH_3CHO, and C_3H_6 over Ag/Al_2O_3

Fig. 5 shows the in situ DRIFTS spectra of Ag/Al_2O_3 at various temperatures in steady states in flowing

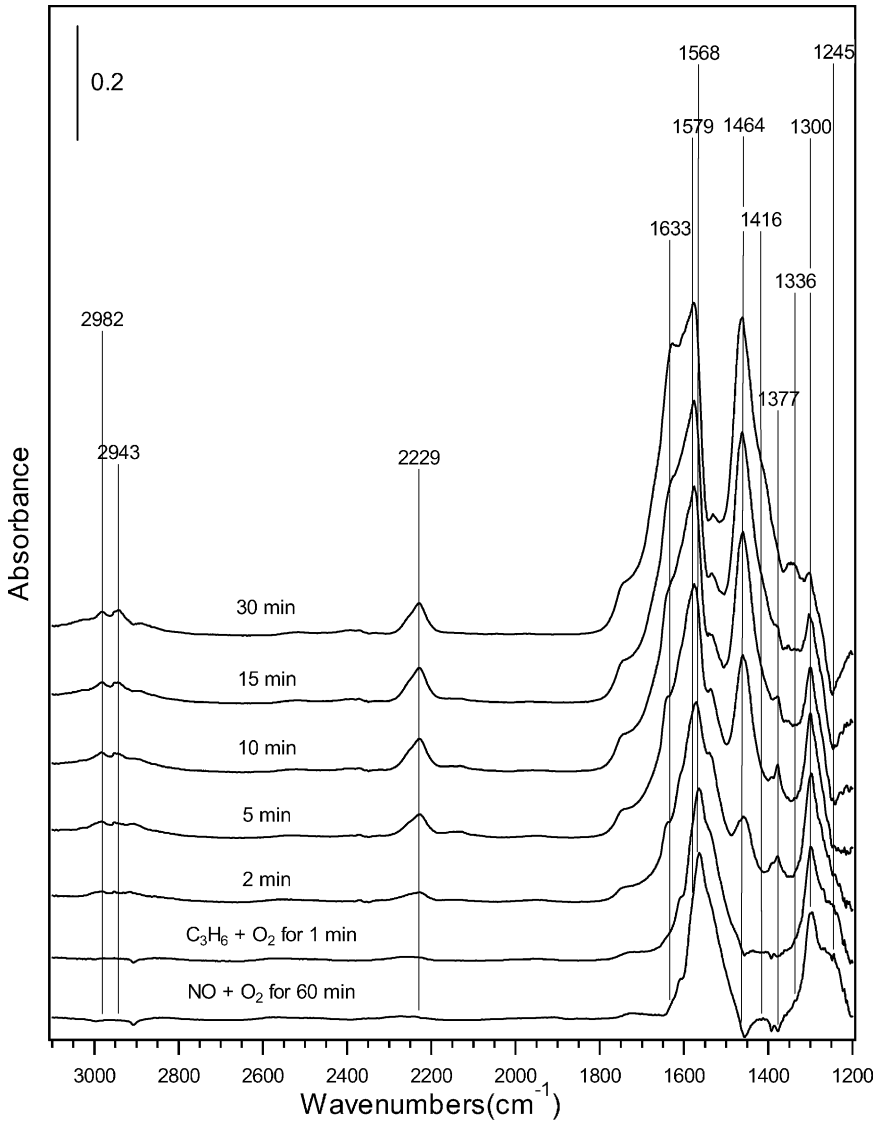

Fig. 4. Dynamic changes of in situ DRIFTS spectra over Ag/Al_2O_3 as a function of time in a flow of $C_3H_6 + O_2$ at 673 K. Before the measurement, the catalyst was pre-exposed to a flow of $NO + O_2$ for 60 min at 673 K. Conditions: NO, 800 ppm; C_3H_6, 1714 ppm; O_2, 10%.

three different gas mixtures: (A) $C_2H_5OH + O_2$, (B) $CH_3CHO + O_2$ and (C) 2,3-dihydrofuran. For C_2H_5OH oxidation (Fig. 5A), two peaks at 1579 and 1466 cm^{-1} were assigned to ν_{as}(OCO), and ν_{as}(OCO) of acetate as the same as in Fig. 2. The peaks at 1633, 1416, and 1336 cm^{-1} were assigned to a surface enolic species, which will be discussed below. Apparently, the enolic species are predominant during the oxidation of C_2H_5OH on the Ag/Al_2O_3 surface within a low temperature range of 473–673 K. At a high temperature range of 773–873 K, however, the surface acetate species become dominant. During partial oxidation of CH_3CHO over Ag/Al_2O_3 (Fig. 5B), the enolic species (peaks at 1633, 1412, and 1336 cm^{-1}) were predominant within the whole temperature region. Heating the sample resulted in an increase in the intensity of acetate peaks (1579 and 1466 cm^{-1}), which was accompanied by a decrease in the intensity of the surface concentration of enolic species. Furthermore, it should be noted that peaks due to ν(C=O) were observed at 1730 and 1759 cm^{-1} [24] within the all temperature region, especially at low temperature region of 473–623 K, indicating that some CH_3CHO molecules did not undergo partial oxidation to form enolic species and acetate.

2,3-dihydrofuran was used to a model compound to confirm the structure of surface enolic species. As shown in Fig. 5C, strong peak at 1630 $cm^{-1}$was also observed, which similarly was accompanied by an appearance of peaks at 1423 and 1315 cm^{-1}. This result strongly supports our assignment about the enolic species. The acetate peaks indicate that partial oxidation of 2,3-dihydrofuran occurred on Ag/Al_2O_3 surface. In addition, peak at 1390 cm^{-1} were observed and assigned to δ(C–H) [24].

The reactivity of the partial oxidation products of C_2H_5OH, formed during $C_2H_5OH + O_2$ reaction over Ag/Al_2O_3 at 673 K, toward $NO + O_2$ was evaluated by the

transient response of DRIFTS method. Fig. 6A shows the dynamic changes of in situ DRIFTS spectra of adsorbed species on Ag/Al_2O_3 in a flow of $NO + O_2$ at 673 K. The integrated areas of these peaks in Fig. 6A were displayed as a function of time in Fig. 6B. After the catalyst was exposed to $C_2H_5OH + O_2$ for 60 min, very strong enolic species peaks at 1633, 1416, and 1336 cm^{-1} and the acetate peaks (1579 and 1464 cm^{-1}) were observed. Switching the fed gas to $NO + O_2$ resulted in a sharp decrease of the intensity of peaks due to enolic species, and then quickly disappeared after 5 min. Simultaneously, a new NCO peak at 2229 cm^{-1} formed, and its intensity promptly increased within 3 min, then decreased. However, the drastic decrease in acetate peak at 1464 cm^{-1} did not occur until the peaks due to enolic species had disappeared nearly. Meanwhile, it was worthwhile to note that large amounts of nitrates and acetate coexisted on Ag/Al_2O_3, whereas the surface concentration of NCO was very low. Taking into account the high reactivity of nitrates toward $C_2H_5OH + O_2$, acetate is not highly reactive toward $NO + O_2$ to form NCO.

The same set of experiments was performed after exposing the catalyst to a flow of CH_3CHO 1565 ppm + O_2 (10%), and similar changes were observed. As shown in Fig. 7A and B, after switching the fed gas to $NO + O_2$ within 10 min, the sharp decrease in the intensity of enolic species peaks was accompanied by a drastic increase in that of NCO peak. After disappearance of the peaks due to enolic species, the intensity of acetate peaks decreased slowly, and a relatively weak NCO peak was observed.

The reactivity of the partial oxidation products of C_3H_6 was evaluated in essentially the same manner as above. After the Ag/Al_2O_3 catalyst was exposed to C_3H_6 1714 ppm + O_2 (10%) for 60 min, only a very weak shoulder at 1633 cm^{-1} was observed (Fig. 8A). As shown in Fig. 8B, switching the

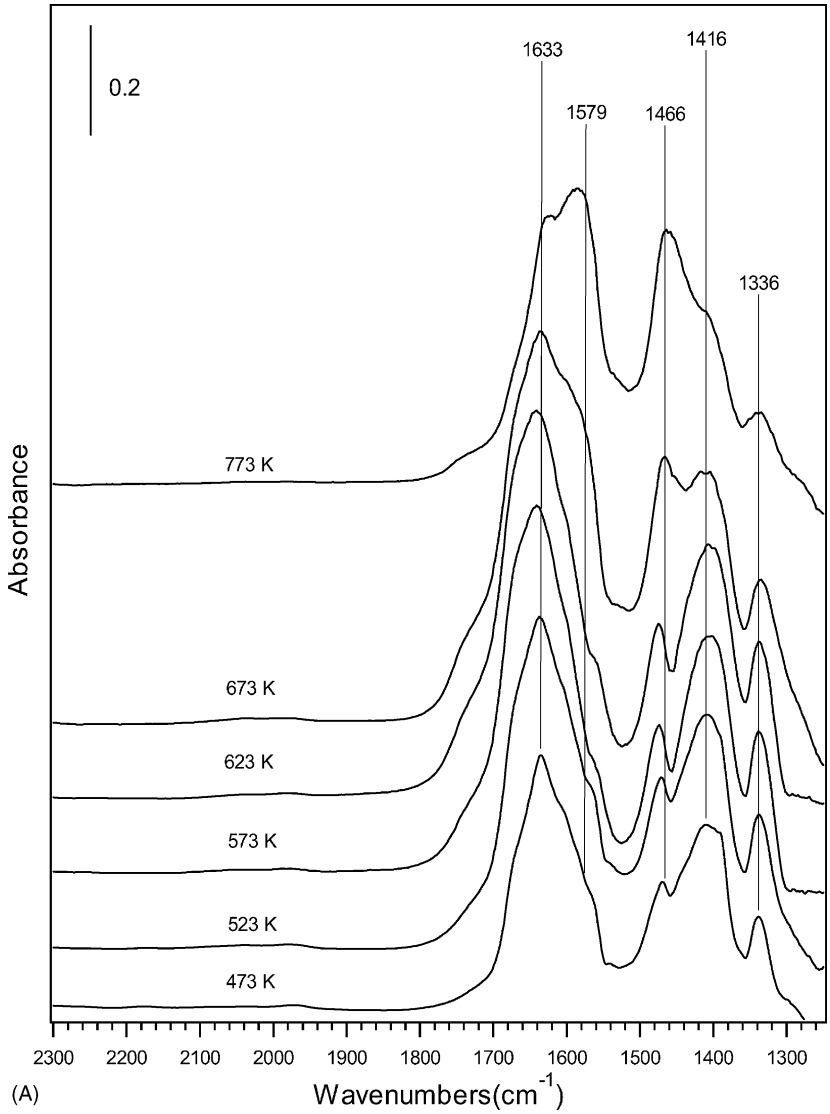

Fig. 5. In situ DRIFTS spectra over Ag/Al_2O_3 in the steady states at different temperatures in a flow of (A) $C_2H_5OH + O_2$, (B) $CH_3CHO + O_2$, and (C) 2,3-dihydrofuran. Conditions: C_2H_5OH, 1565 ppm; CH_3CHO, 1565 ppm; 2,3-dihydrofuran, 1565 ppm; O_2, 10%.

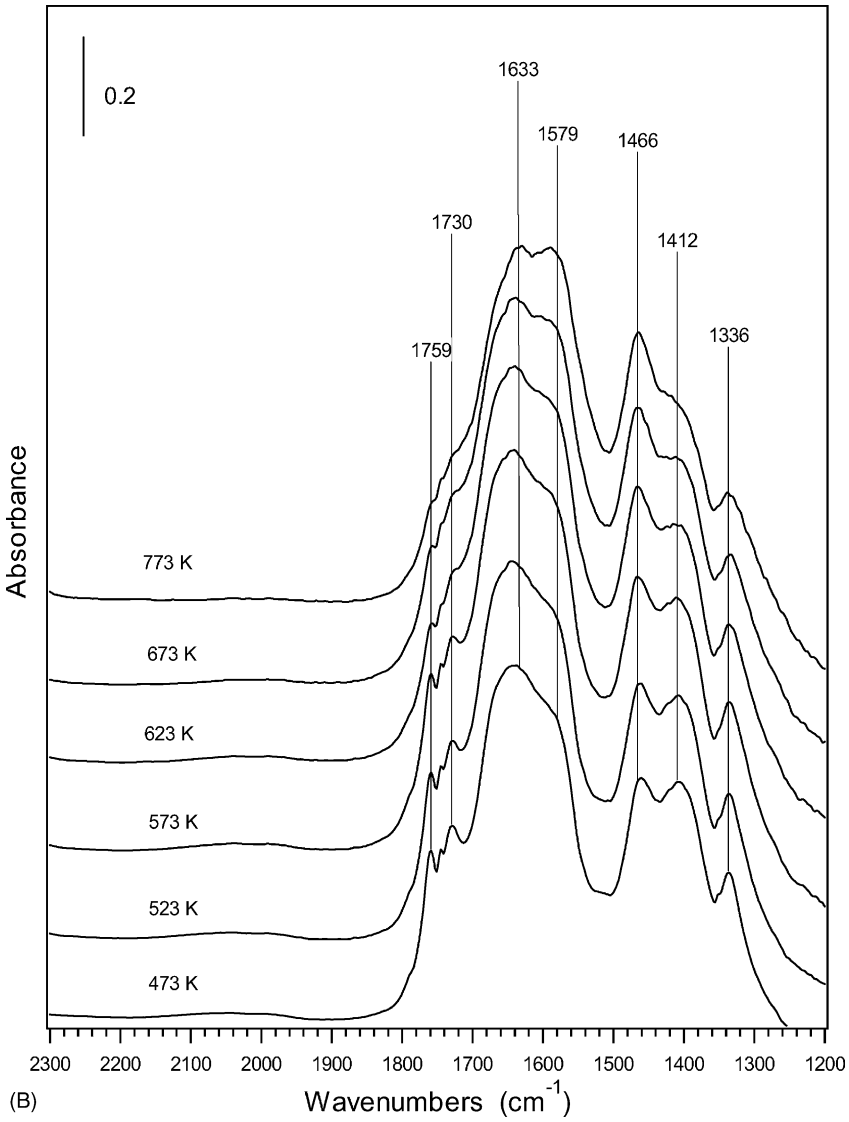

Fig. 5. (*Continued*).

flowing gas to NO + O_2 resulted in similar changes of the enolic species, NCO, acetate, and nitrates.

4. Discussion

4.1. Formation of enolic species

During the partial oxidation of C_2H_5OH, CH_3CHO, and C_3H_6 over Ag/Al_2O_3 at 673 K, peaks at 1633, 1416, and 1336 cm^{-1} were observed. Shimizu et al. [12] reported similar peaks at 1630, 1410, and 1300–1336 cm^{-1} over Ag/Al_2O_3 in flowing *n*-henxane + NO + O_2 and assigned them to carbonate species. Turek et al. [26] reported that when CO_2 chemisorbed on the surface of γ-Al_2O_3, the main adsorbed species were carbonates such as bicarbonates and free carbonates. We also studied the adsorption of CO_2 on Ag/Al_2O_3 at 673 K in flowing CO_2, but no peaks at 1633, 1416, 1336 cm^{-1} were observed even when the concentration of CO_2 in the fed gas was as high as 8%. In addition, the peak at 1633 cm^{-1} was assigned to the stretching vibration model of C=O in formyl species [27] or in aldehyde [28], and OH deformation of adsorbed water was observed at the same position [29].

The peak at 1633 cm^{-1} can be associated with the frequency of double bond stretching vibration, such as ν(C=C) and ν(C=O). In general, however, the stretching vibration frequencies of isolated C=C and C=O should be higher than 1633 cm^{-1}. One evidence is that the IR spectra of syn-vinyl alcohol (CH_2=CHOH) in gas phase, show strong peak between 1644 and 1648 cm^{-1}, which is accompanied by two peaks at 1409–1412 and 1300–1326 cm^{-1} [24,31–33]. The IR spectrum of adsorbed catechol on a TiO_2 colloid also gives a similar peak at 1620 cm^{-1} [25]. Their common characteristic is an enolic structure. We conjecture that in this study, an enolic structure (CH_2=CH–O^-)–M is formed when

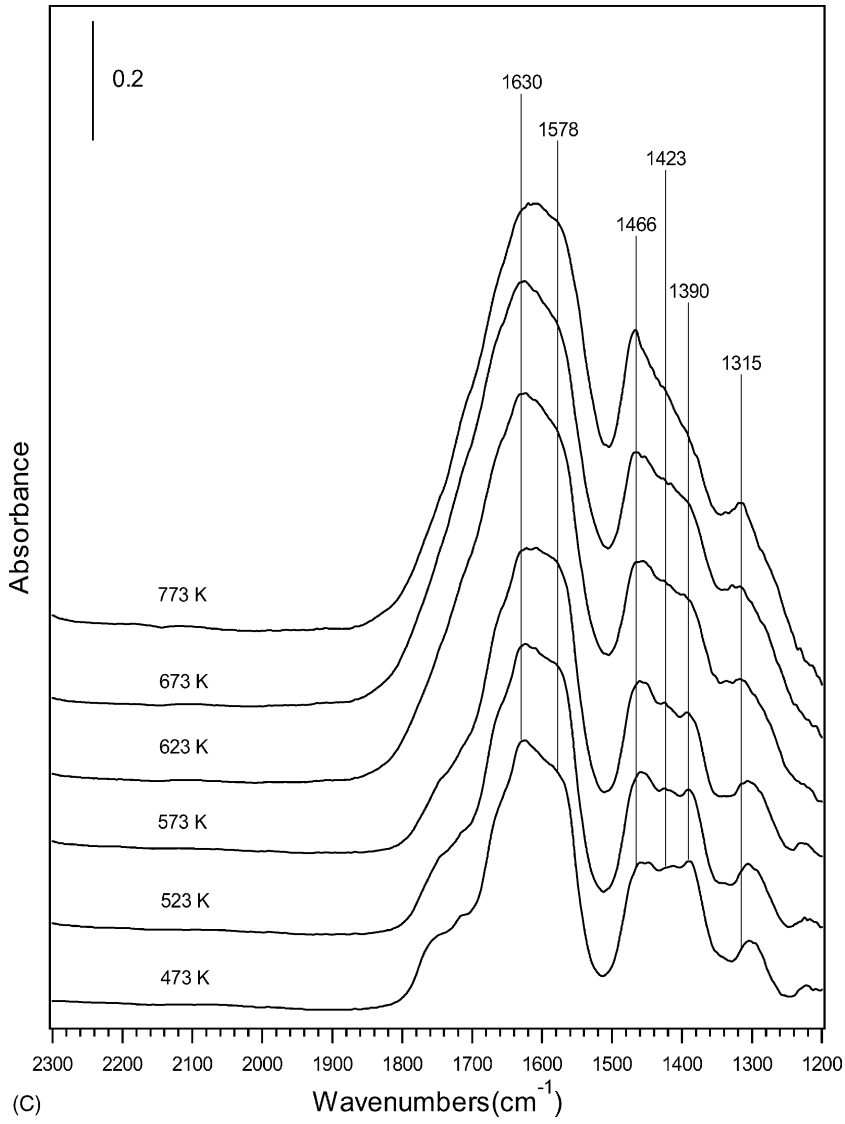

Fig. 5. (*Continued*).

CH_3CHO adsorbs on the surface of Ag/Al_2O_3. The conjugation of CH_2=CH–O^- group may induce the stretching vibrational mode of C=C–O^- to shift to a frequency lower than ν(C=C) and higher than ν(C–O) [24,25]. The peaks between 2872 and 3020 cm^{-1} in Fig. 6A also accord with the distribution of ν(C–H) for a H_2C=CH– group [24,25]. As a consequence, the peak at 1633 cm^{-1} could be tentatively assigned to asymmetric stretching vibration mode of CH_2=CH–O^- group, and peaks at 1416 and 1336 cm^{-1} could be tentatively attributed to symmetric stretching vibration mode of CH_2=CH–O^- and for a C–H deformation mode, respectively [24,30]. Furthermore, similar feature was observed on Ag/Al_2O_3 in exposing to 2,3-dihydrofuran (in Fig. 5C), which has a C=C bonded with an oxygen structure. This result strongly supports our assignments about the surface enolic species. As shown in Fig. 5A and B, when Ag/Al_2O_3 is exposed to $C_2H_5OH + O_2$ and $CH_3CHO + O_2$, very strong peaks at 1633, 1416, and 1336 cm^{-1} are observed, indicating that enolic species are the main surface species. However, these peaks are barely perceptible on Ag/Al_2O_3 in the flow of $C_3H_6 + O_2$ as shown in Fig. 8A, indicating a low surface concentration of CH_2=CH–O^- surface species.

As shown in Fig. 2, during $NO + C_2H_5OH + O_2$ reaction at low temperature region 473–673 K, peak at 1633 cm^{-1} was predominant as well, together with strong peaks at 1416 and 1336 cm^{-1}, indicating that the enolic species are the dominant surface species during the SCR of NO_x by C_2H_5OH over Ag/Al_2O_3 at the low temperature region. Chafik et al. [20] observed a similar peak at 1635 cm^{-1} during $NO + C_2H_5OH + O_2$ over Ag/Al_2O_3, and assigned it to adsorbed organic nitrogen-containing compound. However, in a flow of $C_2H_5OH + O_2$ in Fig. 5A, the peak at 1633 cm^{-1} is absolutely the main peak, which strongly suggests that this peak is due to free-nitrogen species on Ag/Al_2O_3.

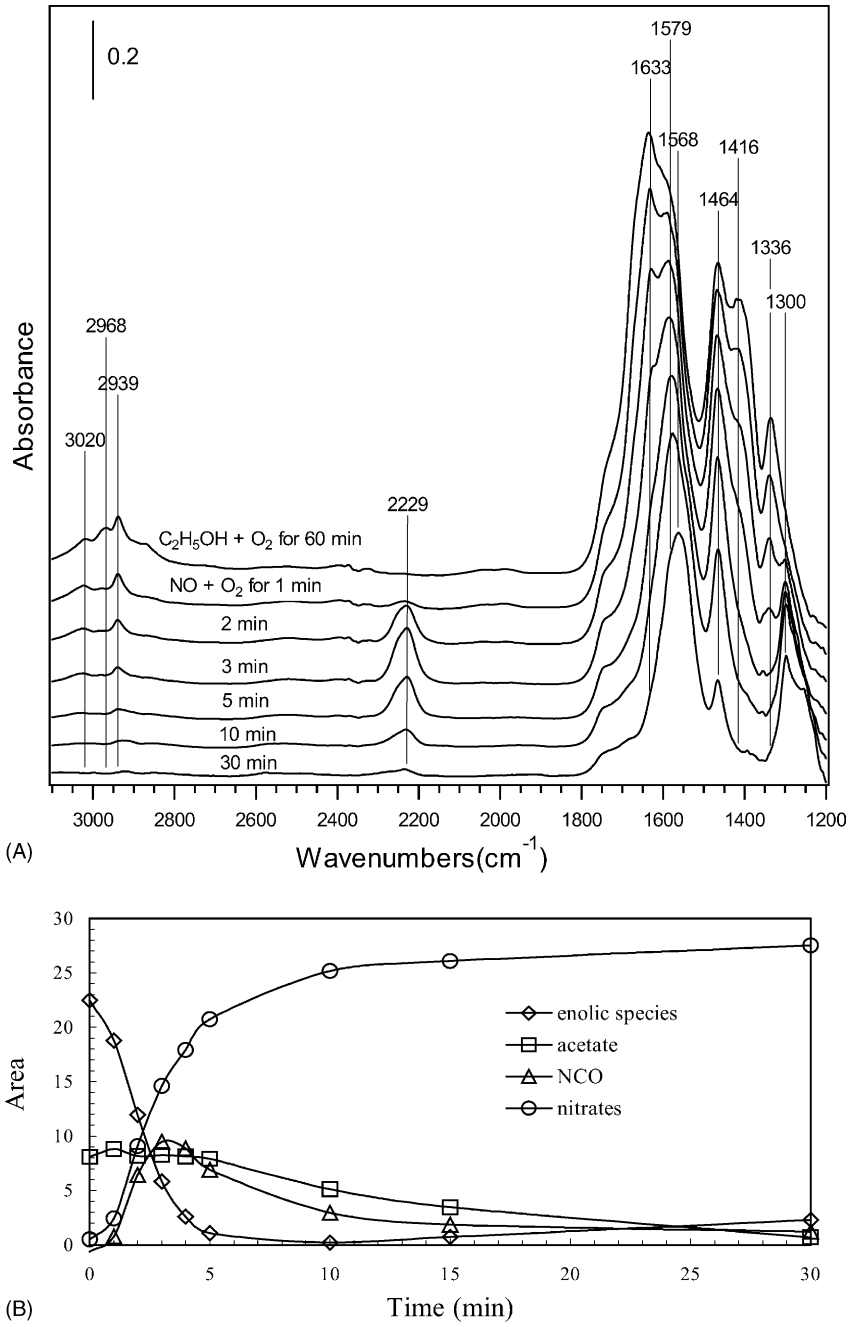

Fig. 6. (A) Dynamic changes of in situ DRIFTS spectra over Ag/Al_2O_3 as a function of time in a flow of $NO + O_2$ at 673 K. Before the measurement, the catalyst was pre-exposed to a flow of $C_2H_5OH + O_2$ for 60 min at 673 K. Conditions: NO, 800 ppm; C_2H_5OH, 1565 ppm; O_2, 10%. (B) Time dependence of the integrated areas of the peak in the range of 2160–2305 cm^{-1} (△, NCO), 1612–1711 cm^{-1} (◇, enolic species), 1439–1508 cm^{-1} (□, acetate) and 1209–1321 cm^{-1} (○, nitrates).

Summarizing the above discussion, the formation of the surface enolic species over Ag/Al_2O_3 can be proposed as shown in Scheme 1.

4.2. Density functional theory calculations

The simulation molecular structure model and FTIR spectrum of the surface enolic species on Ag/Al_2O_3 are shown in Fig. 9A and B. In this model, the enolic species (CH_2=CH–O^-) bond with silver atom, and the optimized distance between the oxygen and silver atom is 2.072 Å. Apparently, the calculated FTIR spectrum is of reasonable similarity to the corresponding experimental result. The asymmetric stretching vibration mode of the enolic species was calculated at 1645 cm^{-1} with a relatively high infrared intensity of 61 km mol^{-1}, which is 12 cm^{-1} higher than the experimental harmonic frequency (1633 cm^{-1}). Compared to the experimental value, the calculated symmetric

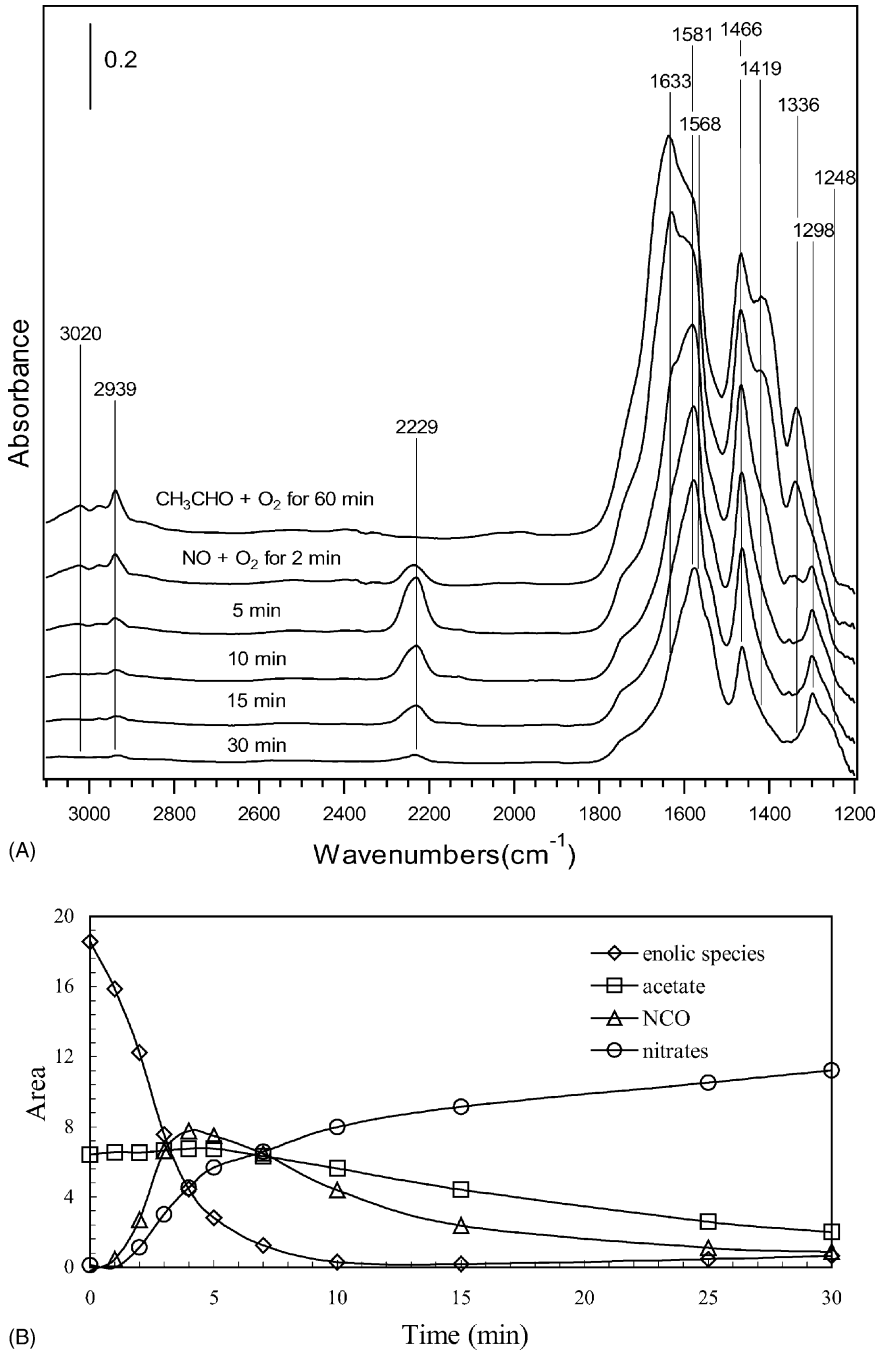

Fig. 7. (A) Dynamic changes of in situ DRIFTS spectra over Ag/Al_2O_3 as a function of time in a flow of $NO + O_2$ at 673 K. Before the measurement, the catalyst was pre-exposed to a flow of $CH_3CHO + O_2$ for 60 min at 673 K. Conditions: NO, 800 ppm; CH_3CHO, 1565 ppm; O_2, 10%. (B) Time dependence of the integrated areas of the peak in the range of 2160–2305 cm^{-1} (△, NCO), 1612–1711 cm^{-1} (◇, enolic species), 1439–1508 cm^{-1} (□, acetate), and 1209–1321 cm^{-1} (○, nitrates).

stretching vibrational mode of this species varied within less than 13 cm^{-1} (1429 cm^{-1} against 1416 cm^{-1}). The calculated C–H deformation vibration mode (1328 cm^{-1}) was 8 cm^{-1} lower than the experimental one (1336 cm^{-1}). On the basis of this result, we conclude that there is excellent agreement between the calculational vibration spectrum and the experimental spectrum, supporting our assignment about the structure of surface enolic species.

4.3. Reactivity of enolic species and acetate

Many research groups have studied the formation and reactivity of acetate during $NO + C_3H_6 + O_2$ reaction on oxide catalysts and metal supported catalysts such as Al_2O_3 [15,16], and Ag/Al_2O_3 [13], and have suggested that the acetate, as a dominant adsorbed species at high temperatures, plays a crucial role in the formation of NCO by reaction

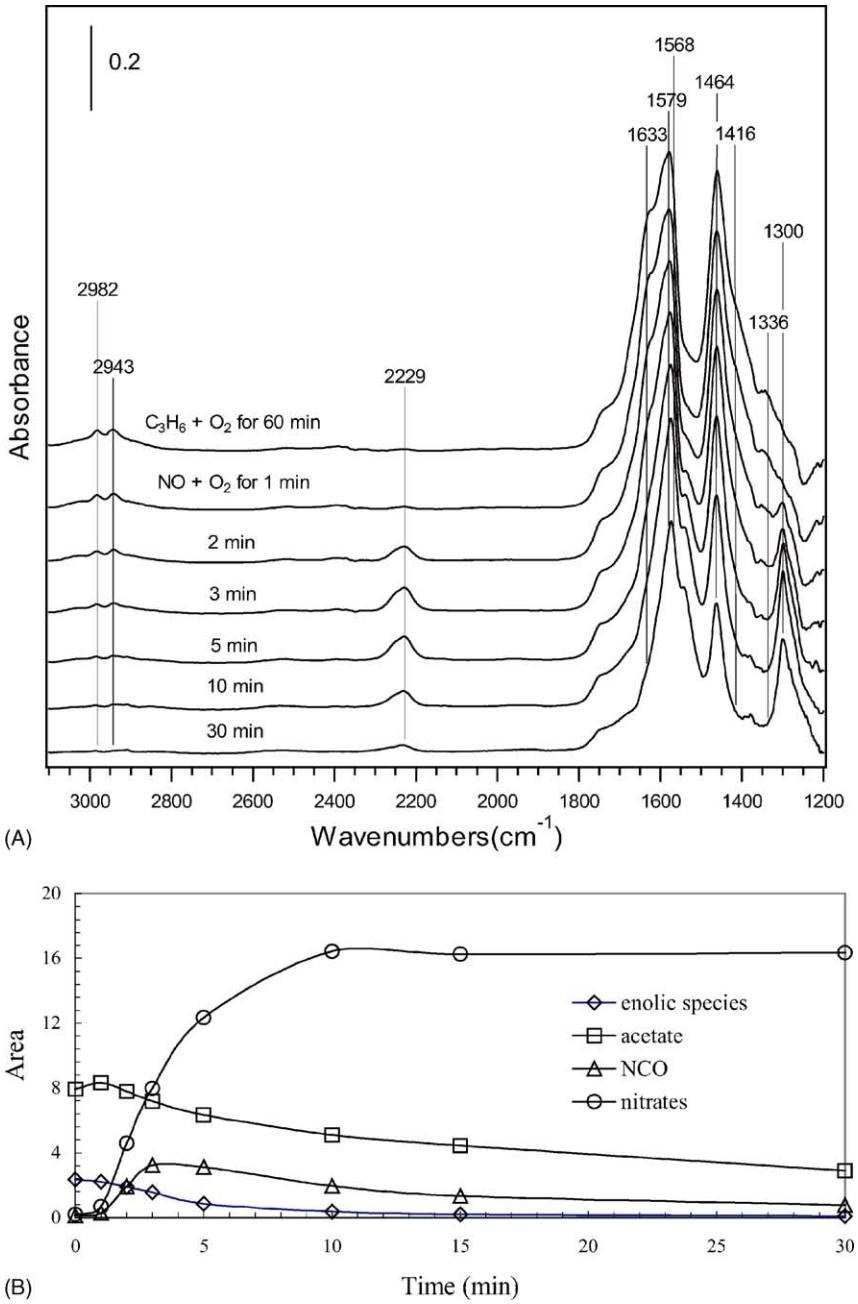

Fig. 8. (A) Dynamic changes of in situ DRIFTS spectra over Ag/Al_2O_3 as a function of time in a flow of $NO + O_2$ at 673 K. Before the measurement, the catalyst was pre-exposed to a flow of $C_3H_6 + O_2$ for 60 min at 673 K. Conditions: NO, 800 ppm; C_3H_6, 1714 ppm; O_2, 10%. (B) Time dependence of the integrated areas of the peak in the range of 2160–2305 cm^{-1} (△, NCO), 1612–1711 cm^{-1} (◇, enolic species), 1439–1508 cm^{-1} (□, acetate), and 1209–1321 cm^{-1} (○, nitrates).

toward $NO+O_2$. In the case of the SCR of NO_x by C_2H_5OH over Ag/Al_2O_3, Kameoka et al. [8] proposed that more acetate and less nitrates were observed in comparison with the SCR of NO_x by C_3H_6, which probably explains why NCO is more easily observed when using C_2H_5OH as a reductant. If the acetate really plays a crucial role in NCO formation during the SCR of NO_x by C_2H_5OH, it should be active for the reaction with $NO + O_2$. However, as shown in Fig. 6, the enolic species have much higher reactivity than acetate on Ag/Al_2O_3 towards $NO+O_2$ to form NCO species. Actually, the acetate did not react with $NO + O_2$ until the enolic species had nearly disappeared on the Ag/Al_2O_3 surface. This means that enolic species, instead of acetate, play a crucial role in the NO_x reduction by C_2H_5OH.

As mentioned above, exposure the sample to $C_2H_5OH + O_2$ for 3 min leads to the complete disappearance of nitrate peaks at 1300 and 1250 cm^{-1} (Fig. 3B), indicating that adsorbed nitrates are highly active in their reaction with $C_2H_5OH+O_2$ to form NCO. However, Fig. 6 shows that after switching the fed gas to $NO+O_2$ for 30 min, strong nitrate

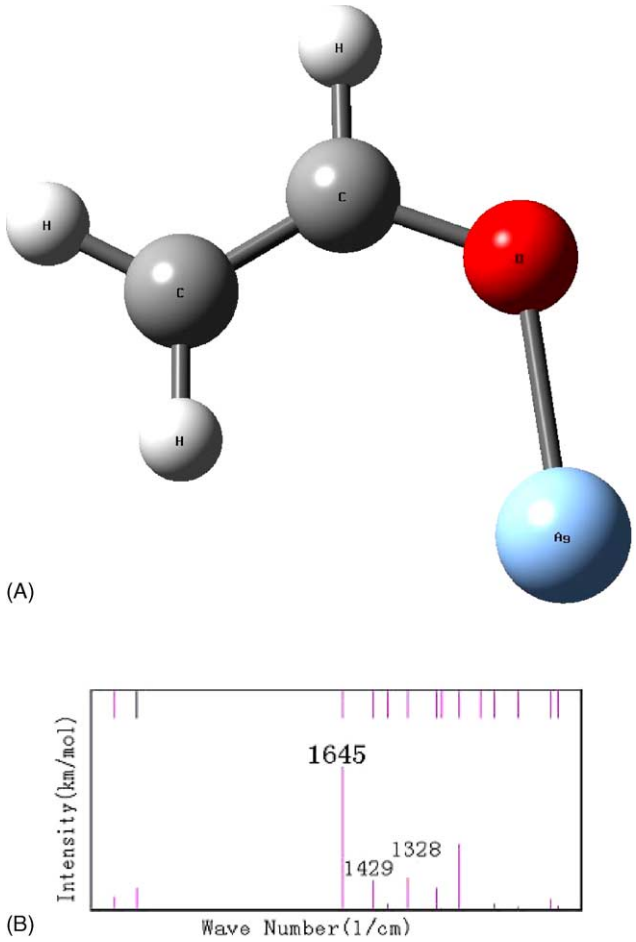

Fig. 9. (A) Molecular structure of the calculational model for the surface enolic species on Ag/Al_2O_3, and (B) calculational FTIR spectrum of the surface enolic species on Ag/Al_2O_3.

and acetate peaks coexisted on the surface of Ag/Al_2O_3, whereas the NCO peak was very weak, which also reveals that acetate is not highly active in its reaction with nitrates to form NCO.

Shimizu et al. [16] have reported that the main adsorption species of CH_3COOH on Al_2O_3 was acetate. We have studied the adsorption of CH_3COOH over Ag/Al_2O_3 and obtained a similar result. As shown in Fig. 1, when using CH_3COOH as a reductant, the highest conversion of NO_x was only 58%. However, when using the same concentration of C_2H_5OH as a reductant, conversion of NO_x was up to 98.7%. Fig. 5 shows that there are only two kinds of partial oxidation products of C_2H_5OH: acetate and adsorbed enolic species, which is additional evidence in favor of our suggestion that enolic species are quite active in their reaction with $NO+O_2$ to form NCO during the SCR of NO_x by C_2H_5OH.

$$\underset{C_3H_6}{C_2H_5OH} \xrightarrow[Ag/Al_2O_3]{\text{oxidation}} CH_3CHO \xrightarrow[Ag/Al_2O_3]{\text{oxidation}} (CH_2{=}CH\text{-}O^-)\text{-}M$$

Scheme 1. The formation of enolic species over Ag/Al_2O_3 from C_2H_5OH, CH_3CHO and C_3H_6.

We already know that there is a correlation between the high efficiency of NO_x reduction by C_2H_5OH and the high productivity of a surface NCO over Ag/Al_2O_3 [5,14,19]. Since enolic species are active in their reaction with $NO+O_2$ to form NCO, and are the predominant surface species during the $C_2H_5OH+O_2$ and the $C_2H_5OH+NO+O_2$ reaction, it is reasonable to expect and obtain a high concentration of surface NCO and high efficiency of NO_x reduction by C_2H_5OH.

In comparison with C_2H_5OH, the same enolic species were obtained during partial oxidation of CH_3CHO. The results of TPO experiments of C_2H_5OH over Ag/Al_2O_3 [34] indicated that CH_3CHO was the main product of partial oxidation of C_2H_5OH. As described above, CH_3CHO is produced from partial oxidation of C_2H_5OH over Ag/Al_2O_3, so using CH_3CHO or C_2H_5OH as reductant has the same efficiency for the SCR of NO_x. Our results in Fig. 1 show that NO_x conversions by C_2H_5OH and CH_3CHO are nearly the same at temperatures below 766 K, which is in good agreement with the suggestion based on our DRIFTS studies. In addition, NO_x conversion by CH_3CHO is relatively lower than that by C_2H_5OH at temperatures above 766 K. It is possible that non-selective oxidation reaction of CH_3CHO in gas phase may occur easily above 766 K, which induces a smaller amount of CH_3CHO to participate in the selective reduction of NO_x.

In the case of partial oxidation of C_3H_6, a small amount of enolic species was formed, accompanied by large amounts of acetate on Ag/Al_2O_3. Therefore, it is reasonable that the efficiency of C_3H_6 for NO_x reduction is much lower than that of C_2H_5OH and CH_3CHO, which has been tested by our results in Fig. 1.

4.4. Mechanism of the SCR of NO_x by C_2H_5OH over Ag/Al_2O_3

On the basis of the results in this work together with the mechanism suggested for the SCR of NO_x by C_3H_6, we propose a simplified reaction scheme for the NO_x reduction by C_2H_5OH. As shown in Scheme 2, the reaction starts with the formation of both adsorbed nitrates via the NO oxidation by O_2 and enolic species and acetate via the partial oxidation of C_2H_5OH over Ag/Al_2O_3. The reaction between the two kinds of adsorbed species then leads to the formation of NCO directly, or via organo-nitrogen compounds (such as R–ONO and R–NO_2), which is widely accepted in the study of the SCR of NO_x [4,8,13,20,35]. Subsequently, NCO reacts with $NO+O_2$ and nitrates to yield N_2. It should be pointed out that the acetate formed by the reaction of $C_2H_5OH+O_2$ also reacts toward $NO+O_2$ to produce NCO. However, the relatively low activity of acetate toward $NO+O_2$ results in this parallel reaction not playing an important role in the formation of NCO.

Obviously, the DRIFTS results for the SCR of NO_x by C_2H_5OH are quite different from previous studies for the SCR of NO_x by C_3H_6. It is worthwhile to point out that this

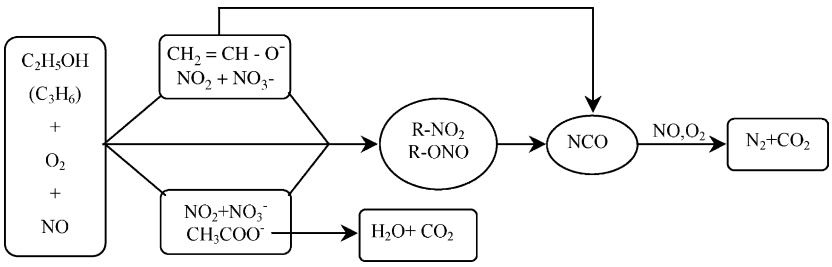

Scheme 2. The possible mechanism of the SCR of NO_x by C_2H_5OH (C_3H_6) over Ag/Al_2O_3.

difference may be induced by sample preparation such as dilution with KBr. We find that DRIFTS spectra are quite different at the same conditions with or without KBr in Ag/Al_2O_3. Our previous work used samples with KBr [4,5], and this work used samples without KBr. The detailed discussion is expected in the next paper.

5. Conclusions

Enolic species, as important intermediate, are formed on Ag/Al_2O_3 during the SCR of NO_x by C_2H_5OH. Both enolic species and acetate are formed over Ag/Al_2O_3 during the partial oxidation of C_2H_5OH, CH_3CHO or C_3H_6 over Ag/Al_2O_3. Peaks at 1633, 1416, 1336 cm^{-1} are assigned to surface enolic species, which are in good agreement with results of DFT calculations. The enolic species have higher reactivity with $NO + O_2$ on Ag/Al_2O_3 than acetate species have. The enolic species are the main surface species during the partial oxidation of C_2H_5OH or CH_3CHO over Ag/Al_2O_3. As a result, high surface concentration of NCO and high efficiency of NO_x reduction are obtained when using C_2H_5OH or CH_3CHO as a reductant during the SCR of NO_x. In contrast, acetate is the main surface species over Ag/Al_2O_3 during the partial oxidation of C_3H_6. This relates to a lower NCO concentration over Ag/Al_2O_3 as well as a relatively lower NO_x conversion when using C_3H_6 as a reductant.

Acknowledgements

This work was financially supported by State Hi-tech Research and Development Project of the Ministry of Science and Technology, Peoples Republic of China (Grant 2001AA643040) and the Chinese Academy of Sciences Program for attracting overseas professionals.

References

[1] T. Miyadera, Appl. Catal. B 2 (1993) 199.
[2] K.A. Bethke, H.H. Kung, J. Catal. 172 (1997) 93.
[3] M.C. Kung, K.A. Bethke, J. Yan, J.-H. Lee, H.H. Kung, Appl. Surf. Sci. 121/122 (1997) 261.
[4] S. Sumiya, H. He, A. Abe, N. Takezawa, K. Yoshida, J. Chem. Soc., Faraday Trans. 94 (1998) 2217.
[5] S. Sumiya, M. Saito, H. He, Q.-C. Feng, N. Takezawa, Catal. Lett. 50 (1998) 87.
[6] T. Nakatsuji, R. Yasukawa, K. Tabata, K. Ueda, M. Niwa, Appl. Catal. B 17 (1998) 333.
[7] F.C. Meunier, J.P. Breen, V. Zuzaniuk, M. Olsson, J.R.H. Ross, J. Catal. 187 (1999) 493.
[8] S. Kameoka, Y. Ukisu, T. Miyadera, Phys. Chem. Chem. Phys. 2 (2000) 367.
[9] K. Shimizu, A. Satsuma, T. Hattori, Appl. Catal. B 25 (2000) 239.
[10] A. Martínez-Arisa, M. Fernández-García, A. Iglesias-Juez, J.A. Anderson, J.C. Conesa, J. Soria, Appl. Catal. B 28 (2000) 29.
[11] F.C. Meunier, J.R.H. Ross, Appl. Catal. B 24 (2000) 23.
[12] K. Shimizu, J. Shibata, H. Yoshida, A. Satsuma, T. Hattori, Appl. Catal. B 30 (2001) 151.
[13] R. Burch, J.P. Breen, F.C. Meunier, Appl. Catal. B 39 (2002) 283.
[14] S. Kameoka, T. Chafik, Y. Ukisu, T. Miyadera, Catal. Lett. 55 (1998) 211.
[15] K. Shimizu, H. Kawabata, A. Satuma, T. Hattori, Appl. Catal. B 19 (1998) L87.
[16] K. Shimizu, H. Kawabata, A. Satsuma, T. Hattori, J. Phys. Chem. B 103 (1999) 5240.
[17] Y. Ukisu, S. Sato, G. Muramatsu, K. Yoshida, Catal. Lett. 11 (1991) 177.
[18] Y. Ukisu, S. Sato, A. Abe, K. Yoshida, Appl. Catal. B 2 (1993) 147.
[19] S. Kameoka, T. Chafik, Y. Ukisu, T. Miyadera, Catal. Lett. 51 (1998) 11.
[20] T. Chafik, S. Kameoka, Y. Ukisu, T. Miyadera, J. Mol. Catal. A 136 (1998) 203.
[21] Y. Yu, H. He, Q. Feng, J. Phys. Chem. B 107 (2003) 13090.
[22] J. Najbas, R.P. Eischens, in: Proceedings of the Ninth International Confrence on Catalysis, vol. 3 1998, p. 1434.
[23] F.C. Meunier, V. Zuzaniuk, J.P. Breen, M. Olsson, J.R.H. Ross, Catal. Today 59 (2000) 287.
[24] Standard IR Spectra, Sadtler Research Labs.
[25] T. Rajh, L.X. Chen, K. Lukas, T. Liu, M.C. Thurnauer, D.M. Tiede, J. Phys. Chem. B 106 (2002) 10543.
[26] A.M. Turek, I.E. Wachs, E. DeCanio, J. Phys. Chem. 96 (1992) 5000.
[27] A. Kiemann, J.P. Hindermann, in: S. Kaliaguine (Ed.), Keynotes in Energy Related Catalysis, vol. 35, Elsevier, Amsterdam, 1988, p. 181.
[28] K. Nakamoto, Infrared and Raman Spectra of Coordination Compounds, Wiley, New York, 1986.
[29] N.W. Hayes, R.W. Joyner, E.S. Shpiro, Appl. Catal. B 8 (1996) 343.
[30] M. Mikami, I. Nakagawa, T. Shimanouchi, Spectrochim. Acta 23A (1967) 1037.
[31] M. Rodler, C.E. Blom, A. Bauder, J. Am. Chem. Soc. 106 (1984) 4029.
[32] Y. Koga, T. Nakanaga, K. Sugawara, A. Watanabe, M. Sugie, H. Takeo, S. Kondo, C. Matsumura, J. Mol. Spectrom. 145 (1991) 315.
[33] D.-L. Joo, A.J. Merer, D.J. Clouthier, J. Mol. Spectrom. 197 (1999) 68.
[34] E.M. Cordi, J.L. Falconer, Appl. Catal. A 151 (1997) 179.
[35] T. Tanaka, T. Okuhara, M. Misono, Appl. Catal. B 4 (1994) L1.